

Constraining accretion-ejection parameters of a newly discovered Galactic transient Swift J151857.0-572147 using *IXPE* and *NuSTAR* observations

SANTANU MONDAL,¹ S. PUJITHA SURIBHATLA,¹ KAUSHIK CHATTERJEE,² CHANDRA B. SINGH,² AND RWITIKA CHATTERJEE³

¹Indian Institute of Astrophysics, II Block, Koramangala, Bengaluru 560034, Karnataka, India

²South-Western Institute For Astronomy Research, Yunnan University, University Town, Chenggong, Kunming 650500, China

³Space Astronomy Group, ISITE Campus, U. R. Rao Satellite Center, ISRO, Bengaluru, 560037, India

ABSTRACT

We study the spectro-polarimetric properties of a newly discovered black hole X-ray binary Swift J151857.0-572147 jointly using *IXPE* and *NuSTAR* observations during March 2024. The analysis of *IXPE* data reports mode-independent polarization degree (PD) 1.34 ± 0.27 and polarization angle (PA) $-13.69^\circ \pm 5.85^\circ$, while the model-dependent analysis gives PD 1.18 ± 0.23 and PA $-14.01^\circ \pm 5.80^\circ$. The joint spectral analysis of the broadband data and *NuSTAR* analysis in isolation constrain the mass of the central black hole between $\sim 9.2 \pm 1.6 - 10.5 \pm 1.8 M_\odot$ and a moderate spin parameter of $\sim 0.6 \pm 0.2 - 0.7 \pm 0.2$ with disk inclination $\sim 38^\circ \pm 9^\circ - 47^\circ \pm 15^\circ$. The power-law photon index and cutoff energy are $2.27 \pm 0.03 - 2.42 \pm 0.05$ and $\sim 40 \pm 7 - 62 \pm 8$ keV, suggesting a transition to the soft spectral state of the source during the observation period. Additionally, the best-fitted halo mass accretion is less compared to the disk mass accretion rate, and a relatively lower corona size of $6-9 r_g$ indicates the same spectral state. The mass outflow rate was also low ($< 3\% \dot{M}_{\text{Edd}}$) during these epochs. The hydrogen column density obtained from the fit is relatively high $\sim 4 - 5 \times 10^{22} \text{ cm}^{-2}$.

Keywords: X-rays: binary stars; accretion; accretion disk; Polarization; Shocks; X-rays: individual: Swift J151857.0-572147

1. INTRODUCTION

Matter accreting onto a black hole (BH) forms an accretion disk consisting mainly of two components, the inner puffed-up region which is known as the so-called corona, and the cold Keplerian disk. The first component upscatters soft photons from the Keplerian disk through inverse Comptonization making them hard (Sunyaev & Titarchuk 1980; Haardt & Maraschi 1993; Chakrabarti & Titarchuk 1995; Done et al. 2007; Mondal & Chakrabarti 2013, and references therein). The same region also launches jet/outflows (Chakrabarti 1999; Chattopadhyay & Das 2007; Mondal & Chakrabarti 2021) and polarizes the radiation depending on its temperature, optical depth, geometry, and inclination (Connors et al. 1980; Sunyaev & Titarchuk 1985). Therefore, the polarization properties such as polarization angle (PA) and degree (PD) of any source depend on both corona properties and the seed photon energies. The variation of PD and PA on the optical depth, disk inclination, and outflows was studied in detail both in theory and using simulation (Dovčiak et al. 2008; Li et al. 2009;

Schnittman & Krolik 2010; Begelman & McKee 1983, and references therein). Therefore, by constraining the corona properties of a system, the PD can be constrained or vice-versa along with the intrinsic parameters of the BH (Krawczynski et al. 2022; Veledina et al. 2023; Kushwaha et al. 2023; Rawat et al. 2023; Poutanen et al. 2023; Jana & Chang 2024; Mondal et al. 2024), making spectro-polarimetric studies important in recent days.

Black Hole X-ray binaries (BHXRBs) show variabilities in their spectral states during the outburst time (Remillard & McClintock 2006). In general, they follow a cycle starting from hard state (HS) when spectra are dominated by hard photons from the corona region to soft state (SS) when spectra are dominated by soft photons from the disk through intermediate states (Homan et al. 2001; Belloni et al. 2005; Remillard & McClintock 2006; Nandi et al. 2012; Debnath et al. 2015; Shui et al. 2021; Jana et al. 2016, and references therein). Sometimes, some of the sources may not follow the cycle for several reasons e.g. lack of supply of matter or lack of viscosity etc. (King 1998; Chakrabarti et al. 2019; Mondal 2020; Mondal et al. 2017). Outbursts that do not go to the SS (Tetarenko et al. 2016, and references therein) or pass through all states are called failed-outburst.

The new Galactic transient Swift J151857.0-572147 was first detected by Swift/XRT as a GRB (GRB 20240303A; Kennea et al. 2024a) in Swift Trigger 1218452¹(GCN 35849). However, its constant bright nature without signs of fading along with its localization in the Galactic plane was later confirmed to be a Galactic transient. From the best localization of the source using XRT immediate on-board localization, the RA, and Dec of the source were found to be RA(J2000) = 15h 18m 57.00s and Dec(J2000) = -57d 21' 47.9" (Kennea et al. 2024b). Follow-up radio observations with the MeerKAT telescope were done (Cowie et al. 2024) at 1.28 GHz (L-band) with a bandwidth of 856 MHz at a flux density of 10 mJy (Carotenuto & Russell 2024) on 04 March 2024 for 15 minutes. The inverted radio spectrum ($f(\nu) \propto \nu^\alpha$, where $\nu \sim +0.5$) with the photon index helped designate the nature of the source as consistent with that of an X-ray binary in the hard state, suggesting it may be a neutron star or a black hole. The Australia Telescope Compact Array (ATCA) followed-up the radio observations on 09 March 2024 for ~ 30 minutes at frequencies 5.5 and 9 GHz simultaneously (Saikia et al. 2024). Their analysis also affirmed that the source was a Galactic black hole. After the ATCA, Swift/XRT performed target of opportunity (ToO) on this source with an exposure of 1000s. It was found that the spectrum is well described by the combination of phenomenological disk black body (DISKBB) and power-law model (POWERLAW) models (Del Santo et al. 2024). These findings also solidified the nature of the source as a black hole. There was INTEGRAL serendipitous detection of the source from 8 to 11 March 2024 (Sguera 2024). As part of the monitoring program of GRBs in optical and NIR wavelengths, the 60 cm Robotic Eye Mount (REM) telescope monitored the source in both these wavelengths (Baglio et al. 2024).

The Swift/XRT spectral modeling of the source reported a column density (N_H) of $5.6 \pm 0.06 \times 10^{22} \text{ cm}^{-2}$ with a power-law photon index (Γ) of 1.78 ± 0.02 (see Kennea et al. 2024a). The negative velocity of an HI absorption line imposes the lower limit on the distance to the source to be $4.48_{-0.47}^{+0.67}$ kpc. While the absence of positive velocity absorption lines towards other sources in the field of the HI absorption for Swift J151857 puts an upper limit on the distance as $15.64_{-0.60}^{+0.77}$ kpc (Burrige et al. 2024). Due to a large uncertainty in distance estimation, we used an average distance of 10 kpc throughout our analysis for this source. Other information like the mass, inclination, and spin have not been reported about the source yet. From our analysis, we report these intrinsic properties of the source for the first time.

The *Imaging X-ray Polarimetry Explorer* (IXPE; Weisskopf et al. 2016) has recently observed several black hole X-ray binaries (BHXRBS) and one of them is Swift J151857. The *NuSTAR* (Harrison et al. 2013) has also observed the source simultaneously. In this paper, therefore, we used both observations to carry out broadband spectral and polarimetric studies of the source to understand the spec-

tral states, accretion properties, and intrinsic parameters of the BH. Along with the corona properties, we have also estimated the mass outflow from this system, that connects the disk-corona-outflow with polarization in a single framework.

The paper is organized as follows: in §2 we discuss the observation and data reduction procedure. In §3, we describe the spectro-polarimetric data analysis results, and finally, we draw our conclusions in §4.

2. OBSERVATION AND DATA REDUCTION

The source Swift J151857 was observed on 18 March 2024 by *IXPE* with exposure time 96 ks and *NuSTAR* observed on 17 and 18 March (hereafter, epochs N1 and N2) with exposures 14 and 9 ks respectively. We present the analysis of the data from both the days in this paper. The corresponding observation IDs are 03250201 (as epoch I), 91001311002 (as epoch N1), and 91001311004 (as epoch N2).

IXPE is an imaging X-ray telescope consisting of 3 polarization-sensitive detector units (DUs) that observe in the 2-8 keV energy range. We obtained the Level-2 event files from the HEASARC archive² which are cleaned and calibrated using standard FTOOLS tasks with the latest calibration files (CALDB 20230526) available in *IXPE* database. For extracting the source region, we select a circular region of 50" for all detectors.

For *NuSTAR* analysis, we considered the observations from 17 and 18 March 2024 and have used the standard NUSTARDAS v1.3.1³ software to extract the data. We generated cleaned event files using the NUIPELINE task and generated the spectra using NUPRODUCTS along with CALDB version 20220331. We considered a region of 60" for the source and 120" for the background using DS9 (Joye & Mandel 2003). Furthermore, we used the *grppha* command to group the data with a minimum of 20 counts in each bin. We used the data of *IXPE* in 2-8 keV and *NuSTAR* data in 3 – 79 keV energy ranges for each respective epoch of observation. For spectral analysis, we used XSPEC⁴ (Arnaud 1996) version 12.12.0.

3. DATA ANALYSIS AND RESULTS

3.1. Model-independent IXPE Analysis

The IXPEOBSSIM software v30.6.3⁵ (Baldini et al. 2022) is used for the polarimetric analysis of the Level-2 IXPE data obtained from the HEASARC archive. The XPSELECT task is used to extract the source event lists. We did not carry out background subtraction for this source since it is very bright with average flux $\sim 1.40 \pm 0.02 \times 10^{-8} \text{ erg cm}^{-2} \text{ s}^{-1}$. The model-independent PCUBE algorithm of the XPBIN task (Kislat et al. 2015) is used to obtain the polarization cube parameters in the 2–8 keV energy range. We also used the

² <https://heasarc.gsfc.nasa.gov/docs/ixpe/archive/>

³ <https://heasarc.gsfc.nasa.gov/docs/nustar/analysis/>

⁴ <https://heasarc.gsfc.nasa.gov/xanadu/xspec/>

⁵ However, we note that a different version of the software gives different results, specifically, a non-detection of polarization using v30.6.4. Therefore, these results are solely based on the above-mentioned version.

¹ <https://gcn.nasa.gov/circulars/35849>

PHA1, PHA1Q and PHA1U algorithms of the XPBIN task to obtain the Stokes I, Q and U spectra of the source. To study any possible energy dependence of these parameters, we grouped the 2 – 8 keV data into four energy bands of 2-3, 3-4, 4-6, and 6-8 keV energy ranges and extracted the polarization parameters. We used a similar approach as discussed in Chatterjee et al. (2023); Mondal et al. (2024). The results of the model-independent polarimetric analysis are summarized in Table 1. The measured PD and PA in 2 – 8 keV are 1.34 ± 0.27 and $-13.69^\circ \pm 5.85^\circ$ respectively. We have also performed energy-dependent PD and PA analyses, which are shown in the left and right panels of Fig. 1 respectively. As it can be observed, the polarization measurements decrease with increasing energy and drop below the MDP₉₉ % above 4 keV. This also gives the PD upper limit (99% confidence level, shown in olive dashed line) of $< 1.54\%$ and $< 4.71\%$ in the 4-6 and 6-8 keV bands. The 1σ confidence contours between PA and PD for different energy bands are shown in Fig. 2, obtained using the PCUBE algorithm.

3.2. Model-dependent IXPE Analysis

For the model-dependent polarization study, we have fitted all Stokes spectra for the epoch I using absorbed POWERLAW+DISKBB model convolved with a constant polarization POLCONST which reads in XSPEC as CONST*TBABS*POLCONST*(POWERLAW+DISKBB). All Stokes spectra for all three DUs in the energy band 2 – 8 keV are fitted simultaneously. The above model gives an acceptable fit with $\chi^2/dof = 1706/1332$. We determine the PA = $-14.01^\circ \pm 5.80^\circ$ and the PD (%) = 1.18 ± 0.23 . Both these values are in excellent agreement with the values obtained from PCUBE algorithm. The neutral hydrogen column density N_H is $5.58 \pm 0.13 \times 10^{22} \text{cm}^{-2}$, obtained from TBABS model. The POWERLAW model photon index (Γ) and disk temperature in DISKBB model are 3.68 ± 0.08 and 0.97 ± 0.02 keV respectively. High values of these two parameters may indicate that the source possibly moved to the soft spectral state during this observation epoch. The confidence contours from the model-dependent analysis are shown in Fig. 3. The solid and dashed contours drawn using XSPEC and PCUBE respectively correspond to 1σ confidence.

3.3. Joint IXPE and NuSTAR Analysis

For the broadband spectral analysis of the source, we performed a joint fitting using the simultaneous observations from IXPE in the 2-8 keV range and NuSTAR in the 3 – 79 keV energy range. We used a CONST component for a cross-calibration factor between NuSTAR and IXPE. The broadband energy range (2 – 79 keV) covered by the spectra of Swift J151857 showed a relatively broad Fe K α line for which a Gaussian component (GAUSS model) is used at ~ 6.4 keV. We included a TBABS (Wilms et al. 2000) component to account for interstellar absorption. The data analysis is also performed using NuSTAR data in isolation as well. We carried out spectral analysis using both relativistic and non-relativistic accretion disk models independently to esti-

mate the accretion parameters as well as the intrinsic parameters of the central BH.

3.4. KERRBB Model

A KERRBB (Li et al. 2005) component is used to characterize the emission from an accretion disk, including relativistic effects. This component models the radiation from a geometrically thin and optically thick accretion disk, as proposed by Novikov & Thorne (1973). The CUTOFFPL component was included to account for the Comptonized emission which originates from the inner hot region of the disk or the corona. The total model reads in XSPEC as CONST*TBABS*(GAUSS+CUTOFFPL+KERRBB). To take into account the calibration issues, as noted for other black hole systems (see e.g. Marra et al. 2023; Podgorný et al. 2023; Cavero et al. 2023), we used the gain_fit command in XSPEC to adjust the response file gains of both telescopes. The same procedures were applied for both the epochs.

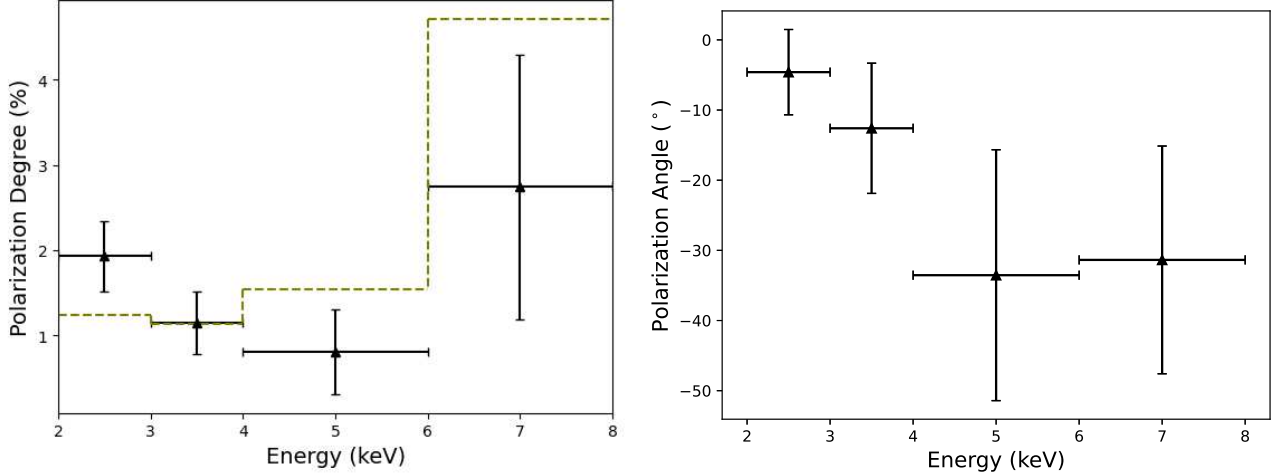
In Fig. 4, we show the model-fitted spectra of Swift J151857 for the joint IXPE and NuSTAR observations. The left and right panels show the spectral fits for the epochs I+N1 and I+N2. The lower panels show the residuals. As we did not have the mass, spin parameters of the BH, and the disk inclination beforehand, we left them free during model fitting, keeping the distance to the source fixed at 10 kpc. However, parameter values may change if the source distance changes significantly. Both data fits returned consistent values of all three parameters in both epochs. The mass (M_{BH}) and spin (a) parameters estimated from the fit vary between $\sim 9.2 \pm 1.6 - 10.5 \pm 1.8 M_\odot$ and $0.60 \pm 0.12 - 0.69 \pm 0.17$ respectively. It possibly indicates that the BH is moderately rotating. The disk inclination (i) and the mass accretion rate obtained from the fit vary between $\sim 38^\circ \pm 9^\circ - 47^\circ \pm 15^\circ$ and $(3.2 \pm 0.5 - 4.0 \pm 0.5) \times 10^{18} \text{gm s}^{-1}$. The low cutoff energy (E_c) of $40 \pm 7 - 62 \pm 8$ keV with a photon index (Γ) of $\sim 2.27 \pm 0.04 - 2.42 \pm 0.05$ indicates a transition to the soft spectral state of the source during the observation epoch after ejecting a high radio flare in the first week of March. The N_H value of the source was high $\sim 3.5 \pm 0.5 - 5.3 \pm 0.4 \times 10^{22} \text{cm}^{-2}$, which can be due to strong outflows from the outer disk or due to the presence of some blobs along the line of sight that can block the central radiation (see Neilsen & Homan 2012; Mondal & Jithesh 2023), requires further study of the outflows from the outer disk. We observed a broad Fe K α width which varies between 0.27 – 0.67 keV. It is expected as the source moved to the soft state, the disk also moved closer to the BH, therefore, relativistic effects can broaden the line (see e.g. Fabian et al. 1989; Iwasawa et al. 1996; Brenneman & Reynolds 2006; Mondal et al. 2016, and references therein). How close has the disk moved inward closer to the BH? What is the corona geometry (radius and height)? This has been studied in the next section.

3.5. JeTCAF Model

To understand the accretion and outflow properties, we have further fitted the data using an accretion-ejection based two-component advective flow (TCAF,

Table 1. Results of model-independent polarimetric analysis performed using PCUBE algorithm.

Parameter	2-3 keV	3-4 keV	4-6 keV	6-8 keV	2 – 8 keV
Q/I (%)	1.90 ± 0.41	1.04 ± 0.37	0.31 ± 0.50	1.25 ± 1.55	1.19 ± 0.27
U/I (%)	-0.30 ± 0.41	-4.92 ± 0.37	-0.75 ± 0.50	-2.43 ± 1.55	-0.61 ± 0.27
PD (%)	1.93 ± 0.41	1.15 ± 0.37	0.81 ± 0.50	2.74 ± 1.55	1.34 ± 0.27
PA ($^\circ$)	-4.60 ± 6.08	-12.60 ± 9.28	-33.54 ± 17.88	-31.36 ± 16.23	-13.69 ± 5.85
MDP ₉₉ (%)	1.24	1.13	1.54	4.71	0.83

**Figure 1.** Energy dependent PD and PA plots in 2 – 8 keV energy range shown with 1σ error bars. The olive dashed line in the left panel represents the estimate of the MDP₉₉%.**Table 2.** Joint *IXPE* and *NuSTAR*, and independent *NuSTAR* spectra of SwiftJ151857 fitted CUTOFFPL+KERRBB model parameters are provided in this table. We have fixed the following parameters: distance $D = 10$ kpc, spectral hardening factor (hd) = 1.7, Gaussian Fe K line energy = 6.4 keV. N_H obtained from both fits is $\sim 4 - 5 \times 10^{22} \text{ cm}^{-2}$.

Model→	KERRBB				CUTOFFPL		GAUSS	χ^2/dof
Epoch	a	i	M_{BH}	\dot{m}_d	Γ	E_c	σ_g	
↓		($^\circ$)	(M_\odot)	($10^{18} \text{ gm s}^{-1}$)		(keV)	(keV)	
I+N1	0.62 ± 0.18	37.6 ± 8.7	9.2 ± 1.6	3.82 ± 0.49	2.42 ± 0.05	61.6 ± 8.4	0.27 ± 0.12	1468/1326
I+N2	0.62 ± 0.08	37.8 ± 6.3	9.7 ± 1.3	4.03 ± 0.47	2.39 ± 0.08	50.1 ± 8.9	0.67 ± 0.13	1177/1145
N1	0.69 ± 0.17	46.9 ± 15.0	10.5 ± 1.8	3.16 ± 0.39	2.27 ± 0.07	48.8 ± 6.7	0.28 ± 0.07	999/890
N2	0.60 ± 0.12	40.1 ± 9.3	9.5 ± 1.4	4.03 ± 0.19	2.27 ± 0.03	40.2 ± 6.5	0.43 ± 0.11	729/709

Chakrabarti & Titarchuk 1995) model including a jet/outflows component (J_{eTCAF} , Mondal & Chakrabarti 2021). The J_{eTCAF} model takes into account the radiation mechanisms at the base of the jet/outflows and the bulk motion effect by the outflowing jet on the emitted spectra, in addition to the Compton scattering of soft disk photons by the hot electron cloud inside the corona. The J_{eTCAF} model has six parameters, namely (i) the mass of the BH (M_{BH}) if it is unknown, (ii) the Keplerian disk accretion rate (\dot{m}_d), (iii) the sub-Keplerian halo accretion rate (\dot{m}_h), (iv) the size of the dynamic corona or the location of the shock (X_s in $r_g = 2GM_{\text{BH}}/c^2$ unit), (v) the shock compression ratio (R),

and (vi) the outflow collimation factor (f_{col}), the ratio of the solid angle subtended by the outflow to the inflow ($\Theta_o/\Theta_{\text{in}}$). The full model reads in *XSPEC* for *IXPE* and *NuSTAR* as `CONST*TBABS*(DISKBB+GAUSS+J_eTCAF)`.

Fig. 5 shows the J_{eTCAF} model fitted spectra for both epochs. The \dot{m}_d and \dot{m}_h values obtained from the fit range between $\sim 0.72 \pm 0.03 - 87 \pm 0.03$ and $\sim 0.23 \pm 0.02 - 0.27 \pm 0.02$. The disk moved much closer to the BH with corona radius $\sim 6-9 r_g$ and $f_{\text{col}} \sim 0.06 \pm 0.01 - 0.08 \pm 0.01$. However, the higher value of \dot{m}_d compared to \dot{m}_h and lower X_s , clearly indicates that the source moved to a soft spectral state. The shock compression ratio (R) varies between $5.4 \pm 0.3 - 6.7 \pm$

Table 3. Joint *IXPE* and *NuSTAR*, and independent *NuSTAR* spectra fitted *DISKBB+JeTCAF* model parameters are provided in this table. All data sets required *GAUSS* model for the Fe $K\alpha$ line ~ 6.4 keV of width σ_g given in the table. N_H obtained from both fits is $\sim 4 - 5 \times 10^{22}$ cm $^{-2}$.

Model→	DISKBB		JeTCAF				GAUSS		χ^2/dof
Epoch ↓	T_{in} (keV)	M_{BH} (M_{\odot})	\dot{m}_d (\dot{M}_{Edd})	\dot{m}_h (\dot{M}_{Edd})	X_s (r_g)	R	f_{col}	σ_g (keV)	
I+N1	0.96 ± 0.01	9.8 ± 1.5	0.74 ± 0.04	0.25 ± 0.01	8.7 ± 1.5	6.67 ± 0.55	0.07 ± 0.02	0.39 ± 0.12	1447/1325
I+N2	0.96 ± 0.01	9.8 ± 1.2	0.72 ± 0.03	0.23 ± 0.02	8.0 ± 1.1	5.41 ± 0.27	0.08 ± 0.01	0.61 ± 0.15	1213/1144
N1	0.97 ± 0.02	9.3 ± 1.3	0.87 ± 0.03	0.27 ± 0.02	6.6 ± 1.1	5.76 ± 0.43	0.06 ± 0.01	0.26 ± 0.08	991/889
N2	0.94 ± 0.02	9.4 ± 1.0	0.83 ± 0.04	0.23 ± 0.02	6.1 ± 1.0	5.46 ± 0.37	0.08 ± 0.02	0.50 ± 0.13	721/708

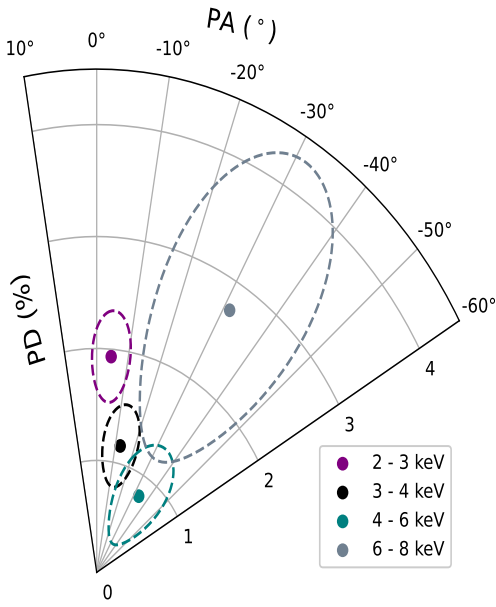


Figure 2. Contour plots between PD and PA obtained using the PCUBE algorithm in 2-3, 3-4, 4-6, and 6-8 keV energy ranges. All contours are drawn with 1σ confidence.

0.6, and falls in the range where the theoretical mass outflow rate is much less (see Chakrabarti 1999). The mass of the BH (M_{BH}) obtained from the fit is 9.3 ± 1.3 and $9.8 \pm 1.5 M_{\odot}$ for both epochs, which are constant within the error bar and also agrees with *KERRBB* model fitted BH mass. All model fitted parameters are given in Table 3.

Given the model fitted parameters, we have estimated the mass outflow rate for this source to be 0.011 ± 0.001 (minimum for I+N1 parameters) and 0.022 ± 0.003 (maximum for N2 parameters) \dot{M}_{Edd} using Eq. 16 derived in Chakrabarti (1999). In our model, as discussed earlier, both the corona and the base of the jet behave as a Comptonizing medium. Such a low mass outflow rate also agrees with the soft spectral state.

4. CONCLUSIONS

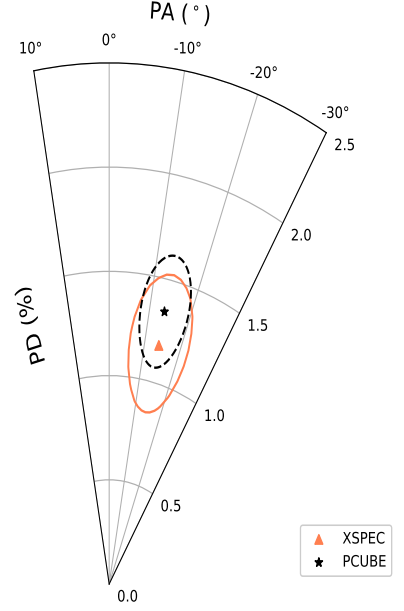


Figure 3. Contour plot between PD and PA with 1σ confidence, obtained using PCUBE algorithm (model-independent) and *XSPEC* (model-dependent) fitting method.

In this paper, we have performed spectro-polarimetric studies of a recently discovered black hole X-ray binary Swift J151857.0-572147 using simultaneous *IXPE* and *NuSTAR* observations during 17 and 18 March 2024. The key findings from this study are summarized below:

- The polarization degree and angle of the source are $\sim 1.34 \pm 0.27\%$ and $\sim -14.0^\circ \pm 5.8^\circ$.
- The low cutoff powerlaw energy ($\sim 40 - 62$ keV) and high powerlaw photon index (2.42 ± 0.05) indicate a transition to a soft spectral state of the source. This is expected as the source ejected a high radio flare in the first week of March and later moved to the soft spectral state.
- Additionally, the high disk mass accretion rate compared to the hot flow rate with lower corona size (\sim

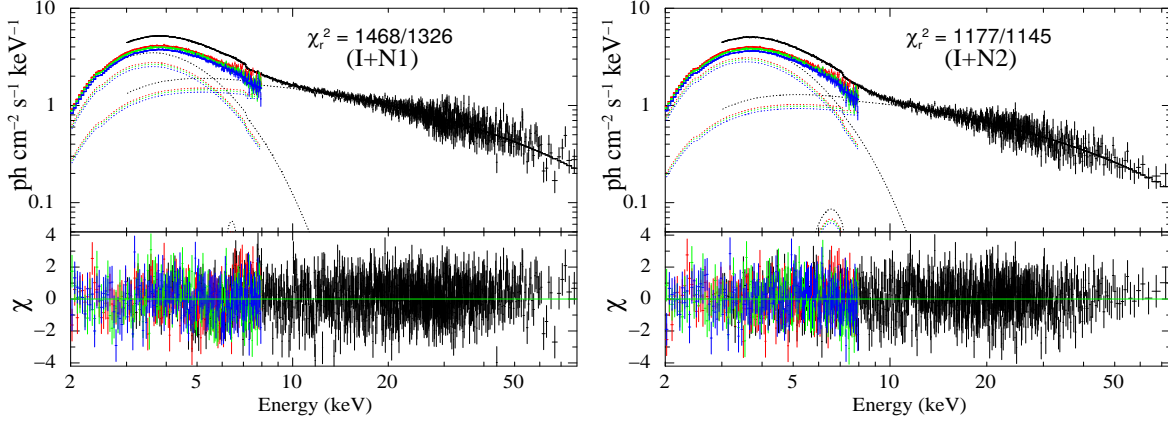


Figure 4. Joint spectral modelling of *IXPE* and *NuSTAR* data fitted using `CUTOFFPL+KERRBB` model in the energy band 2 – 79 keV. The left and right panels are for the epochs (I+N1) and (I+N2). The Fe $K\alpha$ line ~ 6.4 is fitted using `GAUSS` model. The blue, red, and green points correspond to *IXPE* data for all three DUs and the black points correspond to *NuSTAR* data. See the text for details.

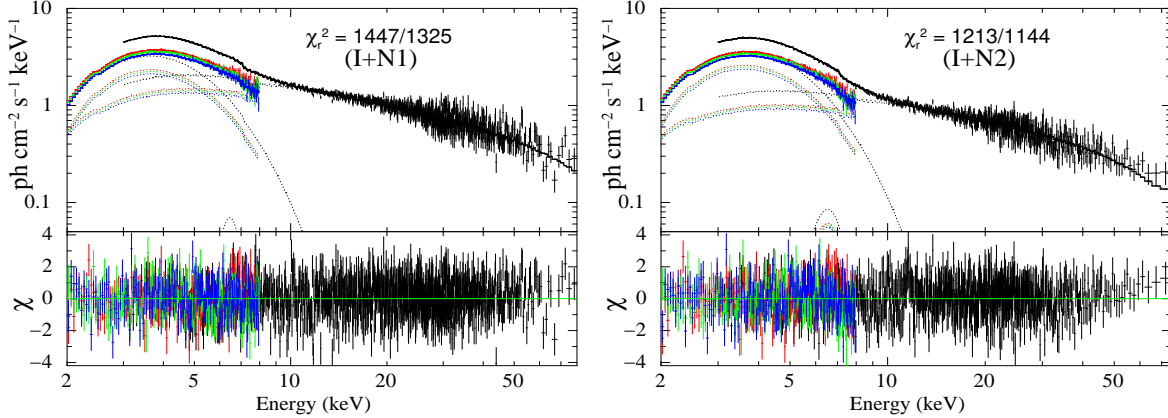


Figure 5. Joint spectral modelling of *IXPE* and *NuSTAR* data fitted using `DISKBB+JeTCF` model in the energy band 2 – 79 keV. The left and right panels are for the epochs (I+N1) and (I+N2). The Fe $K\alpha$ line ~ 6.4 is fitted using `GAUSS` model. The blue, red, and green points correspond to *IXPE* data for all three DUs and the black points correspond to *NuSTAR* data. See the text for details.

$6 - 8 r_g$) also supports the transition of the source to the soft spectral state.

- The mass of the black hole estimated from different model fits in a narrow range between $9.2 \pm 1.6 - 10.5 \pm 1.8 M_\odot$. The spin parameter of the source is $\sim 0.6 \pm 0.2 - 0.7 \pm 0.2$ with accretion disk inclination $\sim 38^\circ \pm 9^\circ - 47^\circ \pm 15^\circ$ for a source distance of 10 kpc.
- We did not find a significant mass outflow rate ($< 0.03 \dot{M}_{\text{Edd}}$), which can be due to the transition of the source to the soft spectral state.

Our detailed study of the BHXRB source SwiftJ151857 sheds light on the accretion disk properties and the geometry of the corona, as well as the estimation of intrinsic properties of the black hole. Moreover, the joint *IXPE* and *NuSTAR*, and independent *NuSTAR* analysis show consistent results. A de-

tailed timing study is required to further confirm the spectral state of the source.

ACKNOWLEDGEMENTS

SM and SPS acknowledge Ramanujan Fellowship (# RJF/2020/000113) by SERB-DST, Govt. of India for this research. K.C. acknowledges support from SWIFAR post-doctoral fund of Yunnan University. CBS is supported by the National Natural Science Foundation of China under grant no. 12073021. This research used data products provided by the *IXPE* Team (MSFC, SSDC, INAF, and INFN) and distributed with additional software tools by the High-Energy Astrophysics Science Archive Research Center (HEASARC), at NASA Goddard Space Flight Center (GSFC). This research has made use of the *NuSTAR* Data Analysis Software (NuSTARDAS) jointly developed by the ASI Science Data Center (ASDC, Italy) and the California Institute of Technology (Caltech, USA).

REFERENCES

- Arnaud, K. A. 1996, *Astronomical Society of the Pacific Conference Series*, Vol. 101, *XSPEC: The First Ten Years*, ed. G. H. Jacoby & J. Barnes, 17
- Baglio, M. C., D’Avanzo, P., Ferro, M., et al. 2024, *The Astronomer’s Telegram*, 16506, 1
- Baldini, L., Bucciantini, N., Lalla, N. D., et al. 2022, *SoftwareX*, 19, 101194, doi: [10.1016/j.softx.2022.101194](https://doi.org/10.1016/j.softx.2022.101194)
- Begelman, M. C., & McKee, C. F. 1983, *ApJ*, 271, 89, doi: [10.1086/161179](https://doi.org/10.1086/161179)
- Belloni, T., Homan, J., Casella, P., et al. 2005, *A&A*, 440, 207, doi: [10.1051/0004-6361:20042457](https://doi.org/10.1051/0004-6361:20042457)
- Brenneman, L. W., & Reynolds, C. S. 2006, *ApJ*, 652, 1028, doi: [10.1086/508146](https://doi.org/10.1086/508146)
- Burridge, B. J., Miller-Jones, J. C. A., Bahramian, A., et al. 2024, *The Astronomer’s Telegram*, 16538, 1
- Carotenuto, F., & Russell, T. D. 2024, *The Astronomer’s Telegram*, 16518, 1
- Cavero, N. R., Marra, L., Krawczynski, H., et al. 2023, *The Astrophysical Journal Letters*, 958, L8, doi: [10.3847/2041-8213/acfd2c](https://doi.org/10.3847/2041-8213/acfd2c)
- Chakrabarti, S., & Titarchuk, L. G. 1995, *ApJ*, 455, 623, doi: [10.1086/176610](https://doi.org/10.1086/176610)
- Chakrabarti, S. K. 1999, *A&A*, 351, 185, <https://arxiv.org/abs/astro-ph/9910014>
- Chakrabarti, S. K., Debnath, D., & Nagarkoti, S. 2019, *Advances in Space Research*, 63, 3749, doi: [10.1016/j.asr.2019.02.014](https://doi.org/10.1016/j.asr.2019.02.014)
- Chatterjee, R., Agrawal, V. K., Jayasurya, K. M., & Katoch, T. 2023, *MNRAS*, 521, L74, doi: [10.1093/mnras/lsad026](https://doi.org/10.1093/mnras/lsad026)
- Chattopadhyay, I., & Das, S. 2007, *New Astronomy*, 12, 454, doi: [10.1016/j.newast.2007.01.006](https://doi.org/10.1016/j.newast.2007.01.006)
- Connors, P. A., Piran, T., & Stark, R. F. 1980, *ApJ*, 235, 224, doi: [10.1086/157627](https://doi.org/10.1086/157627)
- Cowie, F. J., Carotenuto, F., Fender, R. P., et al. 2024, *The Astronomer’s Telegram*, 16503, 1
- Debnath, D., Mondal, S., & Chakrabarti, S. K. 2015, *MNRAS*, 447, 1984, doi: [10.1093/mnras/stu2588](https://doi.org/10.1093/mnras/stu2588)
- Del Santo, M., Russell, T. D., Marino, A., & Motta, S. 2024, *The Astronomer’s Telegram*, 16519, 1
- Done, C., Gierliński, M., & Kubota, A. 2007, *A&ARv*, 15, 1, doi: [10.1007/s00159-007-0006-1](https://doi.org/10.1007/s00159-007-0006-1)
- Dovčiak, M., Muleri, F., Goosmann, R. W., Karas, V., & Matt, G. 2008, *MNRAS*, 391, 32, doi: [10.1111/j.1365-2966.2008.13872.x](https://doi.org/10.1111/j.1365-2966.2008.13872.x)
- Fabian, A. C., Rees, M. J., Stella, L., & White, N. E. 1989, *MNRAS*, 238, 729, doi: [10.1093/mnras/238.3.729](https://doi.org/10.1093/mnras/238.3.729)
- Haardt, F., & Maraschi, L. 1993, *ApJ*, 413, 507, doi: [10.1086/173020](https://doi.org/10.1086/173020)
- Harrison, F. A., Craig, W. W., Christensen, F. E., et al. 2013, *ApJ*, 770, 103, doi: [10.1088/0004-637X/770/2/103](https://doi.org/10.1088/0004-637X/770/2/103)
- Homan, J., Wijnands, R., van der Klis, M., et al. 2001, *ApJS*, 132, 377, doi: [10.1086/318954](https://doi.org/10.1086/318954)
- Iwasawa, K., Fabian, A. C., Reynolds, C. S., et al. 1996, *MNRAS*, 282, 1038, doi: [10.1093/mnras/282.3.1038](https://doi.org/10.1093/mnras/282.3.1038)
- Jana, A., & Chang, H.-K. 2024, *MNRAS*, 527, 10837, doi: [10.1093/mnras/stad3961](https://doi.org/10.1093/mnras/stad3961)
- Jana, A., Debnath, D., Chakrabarti, S. K., Mondal, S., & Molla, A. A. 2016, *ApJ*, 819, 107, doi: [10.3847/0004-637X/819/2/107](https://doi.org/10.3847/0004-637X/819/2/107)
- Joye, W. A., & Mandel, E. 2003, in *Astronomical Society of the Pacific Conference Series*, Vol. 295, *Astronomical Data Analysis Software and Systems XII*, ed. H. E. Payne, R. I. Jedrzejewski, & R. N. Hook, 489
- Kennea, J. A., Lien, A. Y., D’Elia, V., et al. 2024a, *The Astronomer’s Telegram*, 16500, 1
- Kennea, J. A., Lien, A. Y., Page, K. L., & Neil Gehrels Swift Observatory Team. 2024b, *GRB Coordinates Network*, 35853, 1
- King, A. R. 1998, *MNRAS*, 296, L45, doi: [10.1046/j.1365-8711.1998.01652.x](https://doi.org/10.1046/j.1365-8711.1998.01652.x)
- Kislat, F., Clark, B., Beilicke, M., & Krawczynski, H. 2015, *Astroparticle Physics*, 68, 45, doi: [10.1016/j.astropartphys.2015.02.007](https://doi.org/10.1016/j.astropartphys.2015.02.007)
- Krawczynski, H., Muleri, F., Dovčiak, M., Veledina, A., et al. 2022, *Science*, 378, 650, doi: [10.1126/science.add5399](https://doi.org/10.1126/science.add5399)
- Kushwaha, A., Jayasurya, K. M., Agrawal, V. K., & Nandi, A. 2023, *MNRAS*, 524, L15, doi: [10.1093/mnras/lsad070](https://doi.org/10.1093/mnras/lsad070)
- Li, L.-X., Narayan, R., & McClintock, J. E. 2009, *ApJ*, 691, 847, doi: [10.1088/0004-637X/691/1/847](https://doi.org/10.1088/0004-637X/691/1/847)
- Li, L.-X., Zimmerman, E. R., Narayan, R., & McClintock, J. E. 2005, *ApJS*, 157, 335, doi: [10.1086/428089](https://doi.org/10.1086/428089)
- Marra, L., Brigitte, M., Rodriguez Cavero, N., et al. 2023, *arXiv e-prints*, arXiv:2310.11125, doi: [10.48550/arXiv.2310.11125](https://doi.org/10.48550/arXiv.2310.11125)
- Mondal, S. 2020, *Advances in Space Research*, 65, 693, doi: [10.1016/j.asr.2019.08.002](https://doi.org/10.1016/j.asr.2019.08.002)
- Mondal, S., & Chakrabarti, S. K. 2013, *MNRAS*, 431, 2716, doi: [10.1093/mnras/stt361](https://doi.org/10.1093/mnras/stt361)
- Mondal, S., & Chakrabarti, S. K. 2021, *The Astrophysical Journal*, 920, 41, doi: [10.3847/1538-4357/ac14c2](https://doi.org/10.3847/1538-4357/ac14c2)
- Mondal, S., Chakrabarti, S. K., & Debnath, D. 2016, *Ap&SS*, 361, 309, doi: [10.1007/s10509-016-2877-y](https://doi.org/10.1007/s10509-016-2877-y)
- Mondal, S., Chakrabarti, S. K., Nagarkoti, S., & Arévalo, P. 2017, *ApJ*, 850, 47, doi: [10.3847/1538-4357/aa7e27](https://doi.org/10.3847/1538-4357/aa7e27)
- Mondal, S., Chatterjee, R., Agrawal, V. K., & Nandi, A. 2024, *arXiv e-prints*, arXiv:2403.14169, doi: [10.48550/arXiv.2403.14169](https://doi.org/10.48550/arXiv.2403.14169)
- Mondal, S., & Jithesh, V. 2023, *MNRAS*, 522, 2065, doi: [10.1093/mnras/stad1058](https://doi.org/10.1093/mnras/stad1058)
- Nandi, A., Debnath, D., Mandal, S., & Chakrabarti, S. K. 2012, *A&A*, 542, A56, doi: [10.1051/0004-6361/201117844](https://doi.org/10.1051/0004-6361/201117844)

- Neilsen, J., & Homan, J. 2012, *ApJ*, 750, 27, doi: [10.1088/0004-637X/750/1/27](https://doi.org/10.1088/0004-637X/750/1/27)
- Novikov, I. D., & Thorne, K. S. 1973, in *Black Holes (Les Astres Occlus)*, 343–450
- Podgorný, J., Marra, L., Muleri, F., et al. 2023, *MNRAS*, 526, 5964, doi: [10.1093/mnras/stad3103](https://doi.org/10.1093/mnras/stad3103)
- Poutanen, J., Veledina, A., & Beloborodov, A. M. 2023, *The Astrophysical Journal Letters*, 949, L10, doi: [10.3847/2041-8213/acd33e](https://doi.org/10.3847/2041-8213/acd33e)
- Rawat, D., Garg, A., & Méndez, M. 2023, *MNRAS*, 525, 661, doi: [10.1093/mnras/stad2327](https://doi.org/10.1093/mnras/stad2327)
- Remillard, R. A., & McClintock, J. E. 2006, *ARA&A*, 44, 49, doi: [10.1146/annurev.astro.44.051905.092532](https://doi.org/10.1146/annurev.astro.44.051905.092532)
- Saikia, P., Russell, D. M., Baglio, M. C., et al. 2024, *The Astronomer’s Telegram*, 16516, 1
- Schnittman, J. D., & Krolik, J. H. 2010, *ApJ*, 712, 908, doi: [10.1088/0004-637X/712/2/908](https://doi.org/10.1088/0004-637X/712/2/908)
- Sguera, V. 2024, *The Astronomer’s Telegram*, 16524, 1
- Shui, Q. C., Yin, H. X., Zhang, S., et al. 2021, *MNRAS*, 508, 287, doi: [10.1093/mnras/stab2521](https://doi.org/10.1093/mnras/stab2521)
- Sunyaev, R. A., & Titarchuk, L. G. 1980, *A&A*, 500, 167
- . 1985, *A&A*, 143, 374
- Tetarenko, B. E., Sivakoff, G. R., Heinke, C. O., & Gladstone, J. C. 2016, *ApJS*, 222, 15, doi: [10.3847/0067-0049/222/2/15](https://doi.org/10.3847/0067-0049/222/2/15)
- Veledina, A., Muleri, F., Dovčiak, M., et al. 2023, *ApJ Letters*, 958, L16, doi: [10.3847/2041-8213/ad0781](https://doi.org/10.3847/2041-8213/ad0781)
- Weisskopf, M. C., Ramsey, B., O’Dell, S., et al. 2016, in *Society of Photo-Optical Instrumentation Engineers (SPIE) Conference Series*, Vol. 9905, *Space Telescopes and Instrumentation 2016: Ultraviolet to Gamma Ray*, ed. J.-W. A. den Herder, T. Takahashi, & M. Bautz, 990517, doi: [10.1117/12.2235240](https://doi.org/10.1117/12.2235240)
- Wilms, J., Allen, A., & McCray, R. 2000, *ApJ*, 542, 914, doi: [10.1086/317016](https://doi.org/10.1086/317016)